AGU PUBLICATIONS

JGR

Journal of Geophysical Research: Atmospheres

RESEARCH ARTICLE
10.1002/2013JD021396

Key Points:
- CARIBIC observations show overview of tropospheric distributions of CH_3Cl
- Biomass burning/noncombustion sources contribute to the CH_3Cl distributions
- CH_3Cl emitted in South Asia shows a unique biofuel signal

Correspondence to:
T. Umezawa,
taku.umezawa@mpic.de

Citation:
Umezawa, T., A. K. Baker, D. Oram, C. Sauvage, D. O'Sullivan, A. Rauthe-Schöch, S. A. Montzka, A. Zahn, and C. A. M. Brenninkmeijer (2014), Methyl chloride in the upper troposphere observed by the CARIBIC passenger aircraft observatory: Large-scale distributions and Asian summer monsoon outflow, *J. Geophys. Res. Atmos.*, *119*, doi:10.1002/2013JD021396.

Received 19 DEC 2013
Accepted 2 APR 2014
Accepted article online 4 APR 2014

Methyl chloride in the upper troposphere observed by the CARIBIC passenger aircraft observatory: Large-scale distributions and Asian summer monsoon outflow

T. Umezawa[1], A. K. Baker[1], D. Oram[2], C. Sauvage[1], D. O'Sullivan[2,3], A. Rauthe-Schöch[1], S. A. Montzka[4], A. Zahn[5], and C. A. M. Brenninkmeijer[1]

[1]Max Planck Institute for Chemistry, Mainz, Germany, [2]National Centre for Atmospheric Science, Centre for Ocean and Atmospheric Sciences, School of Environmental Sciences, University of East Anglia, Norwich, UK, [3]Now at Met Office, Exeter, UK, [4]Earth System Research Laboratory, NOAA, Boulder, Colorado, USA, [5]Institute for Meteorology and Climate Research, Karlsruhe Institute of Technology, Karlsruhe, Germany

Abstract We present spatial and temporal variations of methyl chloride (CH_3Cl) in the upper troposphere (UT) observed mainly by the Civil Aircraft for Regular Investigation of the atmosphere Based on an Instrument Container (CARIBIC) passenger aircraft for the years 2005–2011. The CH_3Cl mixing ratio in the UT over Europe was higher than that observed at a European surface baseline station throughout the year, indicative of a persistent positive vertical gradient at Northern Hemisphere midlatitudes. A series of flights over Africa and South Asia show that CH_3Cl mixing ratios increase toward tropical latitudes, and the observed UT CH_3Cl level over these two regions and the Atlantic was higher than that measured at remote surface sites. Strong emissions of CH_3Cl in the tropics combined with meridional air transport through the UT may explain such vertical and latitudinal gradients. Comparisons with carbon monoxide (CO) data indicate that noncombustion sources in the tropics dominantly contribute to forming the latitudinal gradient of CH_3Cl in the UT. We also observed elevated mixing ratios of CH_3Cl and CO in air influenced by biomass burning in South America and Africa, and the enhancement ratios derived for CH_3Cl to CO in those regions agree with previous observations. In contrast, correlations indicate a high CH_3Cl to CO ratio of 2.9 ± 0.5 ppt ppb^{-1} in the Asian summer monsoon anticyclone and domestic biofuel emissions in South Asia are inferred to be responsible. We estimated the CH_3Cl emission in South Asia to be 134 ± 23 Gg Cl yr^{-1}, which is higher than a previous estimate due to the higher CH_3Cl to CO ratio observed in this study.

1. Introduction

Methyl chloride (CH_3Cl) is a chlorine-containing trace gas which provides ozone-depleting chlorine (Cl) to the stratosphere [*Montzka et al.*, 2011a; *Santee et al.*, 2013]. Its emissions into the atmosphere mainly originate from natural sources, these being tropical vegetation [e.g., *Yokouchi et al.*, 2000, 2002], biomass burning [e.g., *Lobert et al.*, 1999], oceans [e.g., *Moore et al.*, 1996; *Hu et al.*, 2013], and salt marshes [e.g., *Rhew et al.*, 2000] with a minor contribution by industrial sources [*Keene et al.*, 1999; *McCulloch et al.*, 1999]. Its major sink is via oxidation by hydroxyl radicals (OH) in the troposphere, giving an atmospheric lifetime of ~1 year [*Montzka et al.*, 2011a]. Other minor loss processes include reaction with Cl in the marine boundary layer [*Khalil and Rasmussen*, 1999], uptake by soils [*Khalil and Rasmussen*, 2000], and by polar oceans [e.g., *Moore et al.*, 1996]. In relative terms, CH_3Cl is becoming increasingly important as a Cl supplier to the stratosphere, given that atmospheric abundance of important halogenated species regulated by the Montreal Protocol is declining [e.g., *Montzka et al.*, 2011a]. Considering that the atmospheric CH_3Cl burden is predominantly maintained by natural sources, the response of its emissions to climate change is of special importance. At the same time, monitoring the contribution of anthropogenic emissions is necessary. However, despite progress in using atmospheric chemistry transport models [*Lee-Taylor et al.*, 2001; *Yoshida et al.*, 2004, 2006; *Xiao et al.*, 2010] and isotope measurements [*Keppler et al.*, 2005; *Saito and Yokouchi*, 2008] for quantifying the global CH_3Cl budget, our knowledge of emission strengths of individual sources is far from complete.

Measurements of atmospheric CH_3Cl have shown that the gas has a characteristic spatial distribution. The CH_3Cl mixing ratio is typically about 550 ppt (parts per trillion) in surface air remote from sources and well representative of large regions (baseline air), and it peaks in the tropics, reflecting the presence of strong tropical sources [*Khalil and Rasmussen*, 1999; *Yokouchi et al*., 2000]. Extensive regular measurements have been conducted by the Advanced Global Atmospheric Gases Experiment [*Prinn et al*., 2000], the Halocarbons and other Atmospheric Trace Species Group (HATS) of NOAA/ESRL (Earth System Research Laboratory) [*Montzka et al*., 2011b], the System for Observation of halogenated Greenhouse gases in Europe and by the National Institute for Environmental Studies [*Yokouchi et al*., 2000], providing systematic data sets of atmospheric CH_3Cl at surface baseline sites [see *Xiao et al*., 2010].

Nonetheless, modeling studies indicate that the number of measurement sites is still insufficient to constrain the distribution and magnitude of CH_3Cl sources on regional scales, particularly in the tropics where a major fraction of the global CH_3Cl sources resides [*Lee-Taylor et al*., 2001; *Yoshida et al*., 2004, 2006; *Xiao et al*., 2010]. Because tropical plants as a whole are thought to be the single largest CH_3Cl emitter, observations in the outflow of the important source regions, such as tropical America, tropical Africa, and Asian maritime continents, can effectively constrain estimates of this source and thus contribute to improving the global CH_3Cl budget. However, such measurements are scarce. In addition, since atmospheric transport in the tropics is vertically efficient due to active convection, surface sites at low latitudes often cannot represent regional sources satisfactorily [e.g., *Bousquet et al*., 2011]. In fact, one inverse modeling study suggested that aircraft observation data could provide more powerful constraints on CH_3Cl source estimates than using only surface site data, particularly given that a major part of CH_3Cl sources are located at low latitudes where convective transport is important [*Yoshida et al*., 2006]. In other words, aircraft observations can reveal a footprint of air masses rarely captured by surface measurements and provide a relatively large-scale view of sources with their uneven geographical distribution.

As described earlier, measurements at surface stations have shown variations of CH_3Cl mixing ratios including seasonal/interannual variations and a latitudinal gradient [e.g., *Khalil and Rasmussen*, 1999; *Montzka et al*., 2011b]. In contrast, much less is known about climatological variations of CH_3Cl in the upper troposphere (UT). Although previous campaign-based aircraft observations have shown snapshots of the CH_3Cl distributions over certain regions as discussed later [see *Yoshida et al*., 2004, 2006], they have not enabled larger-scale perspective. In fact, sufficient CH_3Cl data to describe seasonal variations and a latitudinal gradient in the UT as well as a vertical gradient were not available. It is very recent that the HIAPER Pole-to-Pole Observations (HIPPO) project [*Wofsy et al*., 2012] collected extensive CH_3Cl data sets and that the Microwave Limb Sounder on NASA's Aura satellite reported CH_3Cl variations in the UT/lower stratosphere (LS) and the above [*Santee et al*., 2013]. The satellite data indicated strong influences of biomass burning on CH_3Cl variations in the UT and usefulness of CH_3Cl as a dynamical tracer in the stratosphere.

The objective of this study is to characterize large-scale distributions of CH_3Cl mixing ratio in the UT, which is of importance for better understanding the global CH_3Cl budget and also its transport into the stratosphere, but have yet to be documented. The CARIBIC (Civil Aircraft for Regular Investigation of the atmosphere Based on an Instrument Container) observatory [*Brenninkmeijer et al*., 2007] has acquired a large number of CH_3Cl mixing ratio data (and those for a range of other trace gases) using air samples collected monthly along passenger aircraft flight tracks. Using this information and that from surface baseline stations, we highlight the vertical and latitudinal distributions of atmospheric CH_3Cl. Furthermore, the CH_3Cl data are compared to carbon monoxide (CO) data, which helps to disentangle contributions of multiple CH_3Cl sources, because whereas contributions of biomass/biofuel burning elevate both CH_3Cl and CO mixing ratios, other natural sources bring enhancement in CH_3Cl but not in CO. Vegetative emission is known to be the biggest natural global CH_3Cl source, having a flux more than 5 times larger than any of the other individual natural sources (oceans, fungal, and salt marshes) [e.g., *Yokouchi et al*., 2002; *Xiao et al*., 2010]. This dominant source category is referred to as noncombustion sources hereafter. A third factor is that fossil fuel usage enhances CO but not CH_3Cl. Although CH_3Cl has been often used as a tracer for biomass burning [e.g., *Blake et al*., 1996], here we examine contributions of noncombustion sources in shaping its large-scale atmospheric distribution. At the same time, however, we focus on elevated CH_3Cl over South Asia where concomitant CO increases influenced by burning processes were observed in the Asian monsoon plume.

2. Experimental Methods

CARIBIC uses a 1.6 t air freight container with a variety of instruments on board a Lufthansa Airbus A340-600 aircraft (http://caribic-atmospheric.com) [*Brenninkmeijer et al*., 2007]. Four consecutive long-range flights between Frankfurt, Germany, and various destinations have been conducted almost monthly since 2005. In flight, whole air samples are collected in two types of sampling devices named TRAC (Triggered Retrospective Air Collector) housing 2 times 14 glass flasks each and HIRES (High Resolution Sampler) accommodating 88 steel flasks [*Schuck et al*., 2009, 2012]. HIRES was installed in 2010, providing more data coverage in recent years. Nearly all (94%) CARIBIC air samples analyzed for CH_3Cl were collected in the UT/LS region at altitudes of 9–12 km. Here we present part of the data from air samples collected during May 2005–December 2011. The flight destinations during this period included airports in North/South America, South Africa, and South/East Asia [see *Schuck et al*., 2012].

Measurements of CH_3Cl mixing ratio for air samples collected by CARIBIC have been made at the University of East Anglia (UEA) since 2005 and at the Max Planck Institute for Chemistry (MPIC) since 2008, using gas chromatographs coupled with mass spectrometry (GC-MS) and flame ionization detection, respectively [*Krol et al*., 2003; *Baker et al*., 2010]. Measurement precisions are estimated to be ~3% at UEA and ~1% at MPIC. Measurements at UEA are made relative to laboratory standards that are traceable to the NOAA-Global Monitoring Division scale (http://www.esrl.noaa.gov/gmd/ccl/scales.html), and those at MPIC are based on a standard produced by Apel-Riemer Environmental, Inc., which is traceable to standards of National Institute of Standards and Technology (NIST). Overall uncertainties of measurements at UEA and MPIC are estimated to be 5% and 6%. In general, the UEA and MPIC data agree with each other; however, comparison between measurements from both institutes gives a systematic offset of 23 ± 2 ppt (MPIC measurements are lower) and a histogram of the difference has a 1σ width of 36 ppt ($N = 363$). Throughout this paper, we mainly focus on the MPIC data because of the wider data coverage. For comparisons with the NOAA data, the MPIC data are offset by +23 ppt to take into account the above scale difference. The UEA CH_3Cl data from CARIBIC air samples have been partly discussed by *Lai et al*. [2010, 2011].

Results from CARIBIC flights are compared to flask-based measurements conducted by NOAA/ESRL-HATS at multiple surface sites across the globe (data and additional information can be found at ftp://ftp.cmdl.noaa.gov/hats/methylhalides/ch3cl/flasks/). NOAA results from the following four surface sites are considered here: Mace Head (MHD; 53.33°N, 9.90°W, 42 m asl (above sea level)), Mauna Loa (MLO; 19.54°N, 155.58°W, 3433 m asl), American Samoa (SMO; 14.25°S, 170.56°W, 77 m asl), and Cape Grim (CGO; 40.68°S, 144.69°E, 164 m asl) [*Montzka et al*., 2011b]. Samples are collected at MHD and SMO only when winds are from the clean-air sector (wind directions of 180°–335° (west) at MHD and of 330°–160° (east) at SMO). NOAA measurements are made from paired stainless steel or glass flasks filled in parallel using GC-MS techniques. Differences measured in flasks filled simultaneously at these sites are typically ≤0.3% (median) and are ≤1% in 95% of samples collected during the entire measurement record (since the mid- to late-1990s). CH_3Cl mixing ratios are determined against the NOAA scale that is based on eight primary standards prepared gravimetrically at mixing ratios ranging from 260 to 620 ppt. Direct intercomparisons between MPIC and NOAA/ESRL-HATS have not been achieved yet; however, the aforementioned comparison between MPIC and UEA (referenced to the NOAA scale) indicates that the scale difference is small compared to atmospheric variability and thus should not significantly affect the conclusions of this study.

With respect to measurements for other trace gases used in this study, we refer to *Schuck et al*. [2009] for greenhouse gases including nitrous oxide (N_2O), *Brenninkmeijer et al*. [2007] and *Zahn et al*. [2012] for ozone (O_3), and *Scharffe et al*. [2012] for carbon monoxide (CO). Original continuous data for O_3 and CO mixing ratios were averaged over the air sampling periods for direct comparison between different trace gases.

3. Identification of Stratospheric/Tropospheric Air

Commercial aircraft flying at middle- to high-latitudes at typical cruise altitudes of 9–12 km often intersect the tropopause, thereby encountering stratospheric air in association with tropopause breaks and tropopause folds as well as the seasonal and the meridional variability of the tropopause [*Ishijima et al*., 2010]. Stratosphere-troposphere exchange is an important factor affecting trace gas distributions near the tropopause region, especially when the trace gas of interest shows a sharp gradient across the

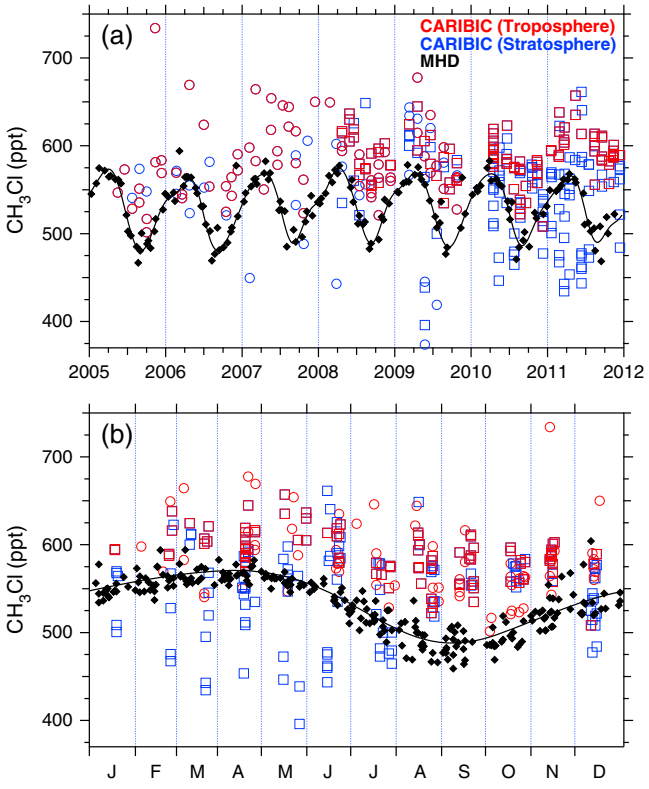

Figure 1. (a) Time series and (b) seasonal variations of the CH_3Cl mixing ratio over Europe observed by the CARIBIC passenger aircraft (open symbols) and NOAA ground-based results from the Mace Head observatory (MHD) (closed black diamonds). Open circles and squares show measurements at UEA and MPIC, respectively. Tropospheric and stratospheric air samples, which were identified based on N_2O mixing ratios, are respectively shown in red and blue. Paired flask results from MHD are fit with a best fit curve (Figure 1a) and average seasonal cycle (Figure 1b) (black solid line).

tropopause [e.g., *Hoor et al.*, 2002]. This is particularly the case for N_2O which is destroyed in the stratosphere (atmospheric lifetime of ~120 year), well mixed in the troposphere, and shows an almost linear atmospheric trend [e.g., *Prinn et al.*, 1990]. As a result, the N_2O mixing ratio decreases above the tropopause, allowing us to identify stratosphere-influenced air [*Ishijima et al.*, 2010; *Assonov et al.*, 2013]. Accordingly, we identified stratospheric air samples in the following manner. The CARIBIC N_2O mixing ratio data were compared with the secular trend observed at MLO [*Hall et al.*, 2007]. MLO N_2O measurements represent baseline air composition in the Northern Hemisphere (NH) troposphere. The MLO trend was deduced by applying a curve fitting technique [*Nakazawa et al.*, 1997] to data obtained by NOAA/ESRL (ftp://ftp.cmdl.noaa.gov/hats/n2o/) [*Hall et al.*, 2007]. If the measured N_2O mixing ratio was more than 1.3 ppb (2 standard deviations) below the MLO trend, the corresponding air sample is classified as stratospheric. This N_2O-based criterion roughly corresponds to a potential vorticity (PV) threshold value of ~2.5 potential vorticity unit (PVU) ($1\ PVU = 10^{-6}\ K\ m^2\ kg^{-1}\ s^{-1}$) defining the dynamical tropopause. We note that this value largely differs from sample to sample because of the relatively coarse resolution of the model for the PV calculation. PV values for this study were calculated using European Centre for Medium-Range Weather Forecasts meteorological data with a horizontal resolution of 1° in latitude and longitude at 6 h time intervals [*van Velthoven*, 2014]. For air samples without N_2O measurements (11% of total), O_3 mixing ratios were used for identifying stratospheric air; the air sample was regarded to be stratospheric if the measured O_3 mixing ratio exceeded the O_3 value at the chemical tropopause varying with season represented by an empirical sine function [*Zahn and Brenninkmeijer*, 2003], which was later confirmed by *Thouret et al.* [2006]. We confirmed that this O_3 tropopause threshold is similar to the N_2O-based criterion. We prefer the use of N_2O over O_3 as a stratospheric tracer because of relatively large tropospheric variability in O_3 [*Assonov et al.*, 2013] and because N_2O is measured from the same air samples for which we analyzed CH_3Cl. During the present observation period May 2005 to December 2011, we identified 1149 stratospheric air samples from 3463 samples in total. It is noted that the frequency at which CARIBIC samples stratospheric air varies with season and latitude due to the different flight routes [*Assonov et al.*, 2013].

4. Observational Results

4.1. Variations Over Europe

Since the CARIBIC aircraft is based in Frankfurt, Germany, the data density for Europe is highest, which allows us to examine temporal variations of CH_3Cl in the UT over Europe (Figure 1). In this figure, data from air samples collected within 10° in latitude and longitude from the Frankfurt Airport (50.03°N, 8.54°E) are plotted for 2005–2011 and for each month. To represent the UT variations, stratospheric air samples were

distinguished in the manner described in section 3. The results are compared in Figure 1 to the NOAA/ESRL-HATS measurements made at a surface site in Ireland, namely, MHD [*Montzka et al*., 2011b].

For the observation period, the CH_3Cl mixing ratio derived from flasks samples in clean air at MHD shows a seasonal cycle with an insignificant secular trend and an annually averaged value of 532 ± 6 ppt for 2005–2011 (Figure 1). The uncertainties shown here and in the following are standard errors of the mean based on standard deviations relative to best fit curves of the data (or simply based on standard errors of the data when the curve fitting is not applied) and do not include the uncertainty of the scale adjustment (see section 2). The seasonal minimum appears in late summer (August–September) and the peak-to-peak amplitude of the seasonal cycle is ~80 ppt (Figure 1b), which is attributable primarily to the seasonal change in OH [*Yokouchi et al*., 2000; *Simmonds et al*., 2004]. The relatively small scatter around the seasonal cycle at MHD indicates the absence of strong local/regional sources in its upwind clean-air oceanic sector. In contrast, the CARIBIC observations show that CH_3Cl in the UT over Europe is characterized by (1) higher values than in the remote lower troposphere (LT) (to be discussed in section 5.1.), (2) a seasonal minimum in late summer as observed in the remote LT, (3) a larger variability than in the remote LT, and (4) frequent encounters of stratosphere-influenced air with low values in winter–spring.

Similar to the surface observations at MHD, a seasonal minimum in late summer is obvious in the UT with a peak-to-peak amplitude of ~60 ppt (Figure 1b). Two factors can contribute to the summertime CH_3Cl minimum in the UT. (1) The highest OH density occurring in summer leads to the late-summer minimum, like for other trace gases reacting with OH. (2) Enhanced vertical transport at NH midlatitudes in summer uplifts CH_3Cl-poor surface air to the UT (see section 5.1 for the vertical gradient of CH_3Cl). The effect of OH has been documented, for instance, in CO over Europe [*Nedelec et al*., 2005], whereas the vertical transport effect causes the opposite seasonal change for gases with higher mixing ratios near the surface such as CO over Asia [*Nedelec et al*., 2005] and CH_4 over northern high latitudes [*Xiong et al*., 2010]. It is also possible that temperature-dependent soil losses of CH_3Cl are enhanced in summer [*Xiao et al*., 2010] and, combined with the vertical transport effect, contribute to the low UT CH_3Cl values.

The third characteristic is that the UT CH_3Cl mixing ratios show higher variability (Figure 1). The MHD station is located in the westernmost part of continental Europe, and the measurements discussed here are collected when clean air arrives from the ocean sector. On the other hand, the CARIBIC data over Europe cover a wider geographical area and pertain to more diverse air mass origins depending on meteorological conditions.

Finally, air masses of stratospheric origin generally show lower CH_3Cl mixing ratios. Most cases occur in winter–spring when CARIBIC aircraft frequently sampled deeper stratospheric air (Figure 1b). In the stratosphere, CH_3Cl is destroyed by reactions with OH, $O(^1D)$, and Cl and also by photolysis. As a result, the CH_3Cl mixing ratio decreases with altitude in the stratosphere as already documented from balloon observations by *Schmidt et al*. [1985] and recent satellite measurements by *Santee et al*. [2013]. Our CARIBIC data around the tropopause indicate a decline of CH_3Cl with decreasing N_2O or increasing height above the tropopause (not shown). At the same time, however, stratospheric air (i.e., low N_2O) having relatively high CH_3Cl mixing ratio has been observed frequently, which may indicate mixing of low-latitude UT air as previously suggested by *Scheeren et al*. [2003a]. It is also noted that we sampled stratospheric air more frequently after 2010. This is primarily because, in the later years, the CARIBIC flights favored routes connecting Frankfurt with northern midlatitude cities such as Vancouver, Canada, Seoul, South Korea, and Osaka, Japan, by which we flew at northern high latitudes more often. This resulted in longer flight time deeper in the stratosphere, even though the aircraft flew at similar pressure levels. In addition, the installation of an additional new stainless steel air sampler (HIRES) after 2010 increased our sampling resolution along the flight tracks, which also has given us more sampling opportunities.

4.2. Variations Over the Atlantic

From April 2009 to December 2011, we frequently carried out CARIBIC flights to Caracas (CCS; 10.60°N, 66.99°W), Venezuela and Bogota (BOG; 4.70°N, 74.14°W), and Columbia, crossing the Atlantic Ocean. The measurements from both flight routes are plotted as a function of time, being binned in 5° latitude bands (Figure 2). As presented in Figure 1, fitting curves for data at midlatitude (MHD) and subtropical (MLO) surface sites are also shown for comparison. The CH_3Cl mixing ratio over the Atlantic shows seasonal variations with minima in late summer over the whole range of observation latitudes. The seasonal cycles are similar in phase

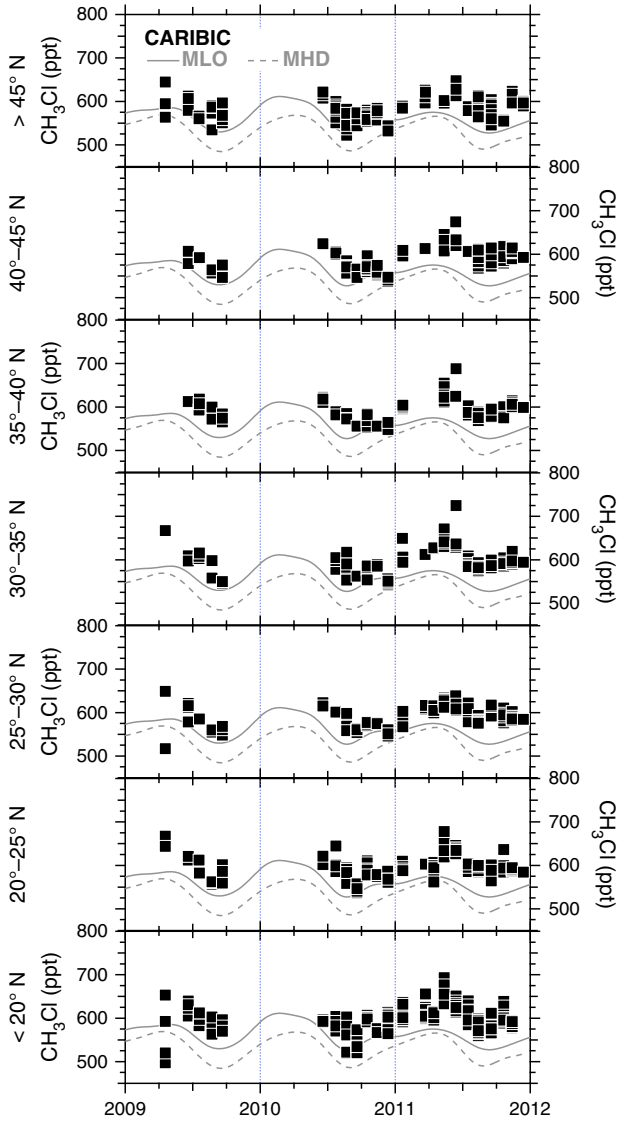

Figure 2. Temporal variations of the CH_3Cl mixing ratio at 5° latitude bins in the UT over the Atlantic. The stratosphere-influenced samples were excluded as described in the text. Fitting curves for NOAA flask measurements at the Mace Head (MHD) and Mauna Loa (MLO) observatories are also shown for comparison.

to those observed at MHD and MLO. As the phase is consistent with the OH loss effect, we suggest that most air samples along the CARIBIC flights over the Atlantic represent the remote atmosphere. Back trajectory analyses [*van Velthoven*, 2014] suggest that the most air samples had been in the UT prevailing westerly flow in the last 8 days. Nevertheless, CARIBIC CH_3Cl is higher than that at MHD throughout the year and comparable or higher than that at MLO, both baseline surface sites. For instance, the annual average value from the CARIBIC flights is 606 ± 8 ppt for the all latitude bins in 2011, while those at MHD and MLO are 532 ± 2 and 560 ± 2 ppt, respectively. Noteworthy is that the CH_3Cl level at MLO (solid line) is higher than that at MHD (dashed line) throughout the year, reflecting a latitudinal gradient of CH_3Cl in the LT peaking in the tropics [*Khalil and Rasmussen*, 1999; *Yokouchi et al.*, 2000].

It is useful to compare CH_3Cl with CO as an indicator of pollution events. In the Atlantic region, we observed high CH_3Cl values accompanied by extremely high CO in June 2011 (red dots in Figure 3), indicative of contributions from biomass burning. We selected air samples with elevated mixing ratios of both CH_3Cl and CO in this month, which appeared around 35°N, the subset of data giving a slope of CH_3Cl against CO of 0.61 ± 0.05 ppt ppb^{-1} ($R^2 = 0.95$, $N = 9$) (Figure 3c). We also observed concomitant enhancements in mixing ratios of biomass burning-related trace gases, such as ethane (C_2H_6) and ethyne (C_2H_2), which, respectively, range from 1350 to 1830 ppt and from 200 to 360 ppt for these air samples. Back trajectory analyses do not show any contact with LT air in the preceding 8 days [*van Velthoven*, 2014], thus preventing us from identifying the geographical origin of the biomass burning events. In this month, we also observed an increasing trend of the CH_3Cl mixing ratio south of 15°N without CO increase. These data form another branch of high CH_3Cl without CO enhancement on the scatterplot (Figure 3c), indicating contributions from noncombustion sources. Back trajectories for these air samples suggest contact to the LT over northern Brazil/Venezuela. Emissions from tropical rainforest in South America [*Gebhardt et al.*, 2008] may explain the elevated CH_3Cl mixing ratios. Measurements in March 2011 (blue squares in Figure 3) also show concomitant increases in CH_3Cl and CO mixing ratios south of 15°N, giving a slope of CH_3Cl over CO of 0.93 ± 0.17 ppt ppb^{-1} ($R^2 = 0.78$, $N = 9$). Back trajectories indicated that these air masses had passed over areas with active fires in Columbia and Venezuela (https://firms.modaps.eosdis.nasa.gov/firemap/). In May 2011, we observed elevated CH_3Cl mixing ratios especially south of 25°N, but these samples were not accompanied by CO enhancements (orange diamonds in Figures 3a–3c), suggesting that noncombustion sources played a substantial role for this period. Back trajectory analyses do not indicate specific areas where those air masses contacted the LT [*van Velthoven*, 2014].

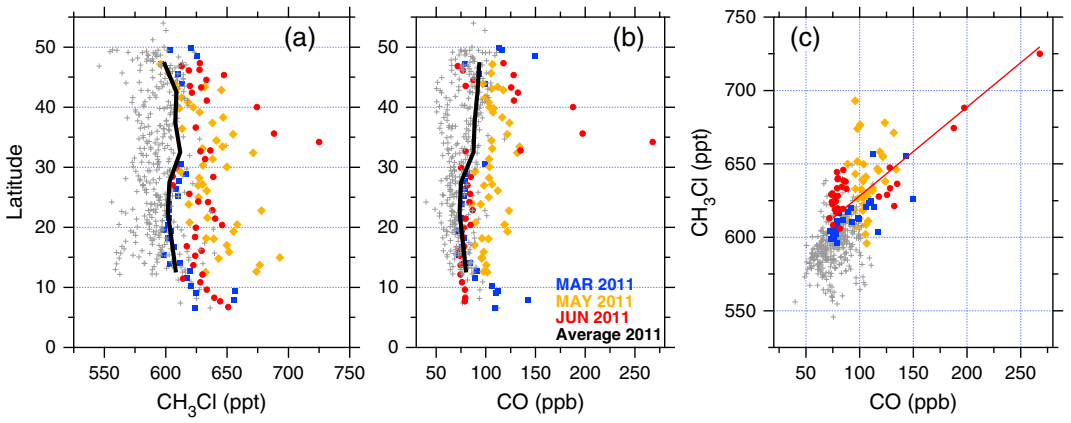

Figure 3. Latitudinal distributions of the (a) CH_3Cl and (b) CO mixing ratios in the UT over the Atlantic for data obtained in 2011. Annual average profiles are shown by black solid lines, and measurements from flights with elevated mixing ratios are highlighted by colors (data from the other flights are shown by gray crosses). (c) A scatterplot between the CH_3Cl and CO mixing ratios. A geometric mean regression line for subset of the June 2011 data is also shown.

It should be noted that the calculated $\Delta CH_3Cl/\Delta CO$ ratio described above might have been slightly overestimated compared to the original emission ratio at the source, since CO reacts with OH faster than CH_3Cl during transport from the source to the observation locations. As discussed previously [*Scheeren et al.*, 2002], for instance, the $\Delta CH_3Cl/\Delta CO$ ratio is expected to increase by ~10% during transport time of about a week, given reaction constants of CH_3Cl and CO with OH [*Sander et al.*, 2011] as well as the summertime average OH concentration in the LT [*Spivakovsky et al.*, 2000]. The potential 10% overestimation still falls within the regression error derived from the original data (Table 1), suggesting a relatively minor effect from chemical loss during transport. Another factor potentially altering the $\Delta CH_3Cl/\Delta CO$ ratio is mixing with air masses that have totally different CH_3Cl to CO signatures, which is, however, more difficult to quantify. In this study, we therefore consider the calculated enhancement ratios representing the emission ratios at the source. The $\Delta CH_3Cl/\Delta CO$ ratio for biomass burning in South America estimated from the Atlantic data agrees with results from previous aircraft measurements (Table 1).

Table 1. Enhancement Ratios of CH_3Cl Relative to CO for Biomass/Biofuel Burning

Region[a]	Observation Date	Enhancement Ratio (ppt ppb^{-1})	Reference[b]
	South America		
Columbia/Venezuela	March 2011	0.93 ± 0.17	This study (BOG)
Brazil	September–October 1992	0.85 ± 0.06	*Blake et al.* [1996]
Brazil/Venezuela	March 1998	1.1 ± 0.2	*Andreae et al.* [2001]
	Africa		
Central East Africa	March 2009	0.49 ± 0.17	This study (CPT)
Central East Africa	January 2011	0.70 ± 0.07	This study (JNB)
Central East Africa	February 2011	0.72 ± 0.07	This study (CPT)
Central East Africa	March 2011	0.73 ± 0.08	This study (CPT)
Southern East Africa	November 2010	0.82 ± 0.16	This study (JNB)
West Africa	February 1991	0.50 ± 0.03	*Rudolph et al.* [1995]
Southern Africa	August–October 1992	0.95 ± 0.01	*Andreae et al.* [1996]
Zambia/Zimbabwe	September–October 1992	0.57 ± 0.03	*Blake et al.* [1996]
	South Asia		
South Asia	June–September 2008	2.9 ± 0.5	This study (MAA)
South Asia	February–March 1999	1.74 ± 0.21	*Scheeren et al.* [2002]
	Laboratory		
Miscellaneous fuels	November 1987 to March 1989	0.18–4.4	*Lobert et al.* [1991]

[a]For this study, the regions where the air masses had contacted the lower part of the atmosphere (< 850 hPa) as traced by back trajectory analyses [*van Velthoven*, 2014].
[b]Flight destinations are shown in parenthesis for this study.

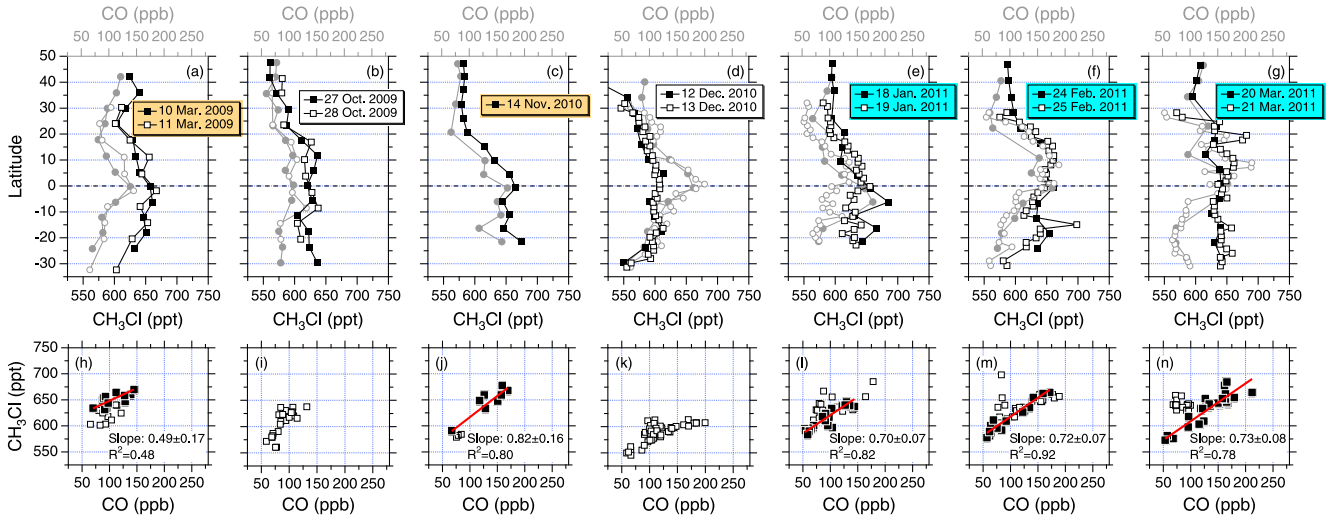

Figure 4. (a–g) Latitudinal distributions of the CH_3Cl (black) and CO (gray) mixing ratios obtained in the UT along CARIBIC flights from/to Cape Town (CPT) and Johannesburg (JNB), South Africa. (h–n) Scatterplots between CH_3Cl and CO for the respective flights. According to back trajectory analyses, air samples influenced by biomass burning are shown by closed squares, while those influenced by noncombustion sources (vegetation and urban sources) are indicated by open symbols. Also shown in red are geometric mean regression lines for the biomass burning samples. The flights influenced by biomass burning and by both biomass burning and vegetation sources are highlighted with the annotation boxes in light orange and light blue, respectively.

It is also noted that CO produced by oxidation of biogenic hydrocarbons, which is a source comparable in strength to biomass burning in the global CO budget [e.g., *Holloway et al.*, 2000], can potentially affect $\Delta CH_3Cl/\Delta CO$ ratios. Colocated CH_3Cl- and hydrocarbon-emitting vegetation could cause correlations between CH_3Cl and the secondary CO. To examine this possibility, we also plotted CH_3Cl data against C_2H_2, which is an exclusive combustion indicator. We found that patterns in the CH_3Cl-C_2H_2 scatterplots are very similar to those in the CH_3Cl-CO scatterplots (not shown). This indicates that the observed correlations with CO are due to combustion sources and that the role of the secondary CO on $\Delta CH_3Cl/\Delta CO$ ratios is minor. In addition, we also note that biogenic hydrocarbons are emitted from most plants [e.g., *Guenther et al.*, 2006], whereas only specific plant types are known to emit CH_3Cl [*Yokouchi et al.*, 2007; *Saito et al.*, 2008; *Blei et al.*, 2010], i.e., namely, not all forested areas emit CH_3Cl.

4.3. Variations Over Africa

In 2009–2011, seven sets of CARIBIC flights between Germany and Cape Town (CPT; 33.96°S, 18.60°E) or Johannesburg (JNB; 26.12°S, 28.24°E), South Africa, took place. All these flights were conducted from October to March and thus do not allow time series analyses covering the whole year. Figure 4 shows latitudinal distributions of the CH_3Cl (black) and CO (gray) mixing ratios over Africa. The CH_3Cl mixing ratio shows a southward increase in the NH during all flights, while in the Southern Hemisphere (SH) it decreases or remains high going south. We recall that this negative northward gradient in the NH was not obvious over the Atlantic (Figure 3), indicating that the UT air over Africa is under strong influence of CH_3Cl sources during these months.

The CO mixing ratio shows clear enhancements around the equator (March 2009, December 2010, and January–March 2011) and south of the equator (November 2010). Three different types of correlations between CH_3Cl and CO were observable in our measurements over Africa. In March 2009, concomitant CH_3Cl and CO increases around the equator were observed (Figure 4a). Back trajectory analyses indicate that air masses had passed over central East Africa where many fires occurred in the preceding week. Also, the air masses with enhanced CH_3Cl and CO values in November 2010 (Figure 4c) had passed over fires in southern East Africa [*van Velthoven*, 2014]. Our measurements show that these air samples from both flights had high mixing ratios of other biomass burning-related trace gases (not shown) [see *Schuck et al.*, 2012]. The measurements from flights in January–March 2011 (Figures 4e–4g) show both biomass burning and noncombustion signatures. During these flights, the air masses around the equator showing high values for both CH_3Cl and CO passed over central East Africa where fires were active at that time. On the other hand, the

CH_3Cl mixing ratio remained high over Southern Africa while the CO decreased moving south. These air masses had passed over Madagascar and eastern Southern Africa [*van Velthoven*, 2014]. The dominant vegetation in the region is deciduous forest [*Mayaux et al*., 2004], and fire activity was low in the season. These data deviated from biomass burning samples on the scatterplots (open symbols in Figures 4l–4n). Noncombustion emissions contributed these elevated CH_3Cl values without CO enhancements. The other case was found in December 2010 (Figure 4d). During this flight, high CO mixing ratios were observed around the equator, while CH_3Cl remained relatively low. Back trajectories indicate that the air masses had passed over southwestern Africa [*van Velthoven*, 2014]. As fire was not active in the region, emissions due to fossil fuel use might explain the observed high CO and low CH_3Cl mixing ratios. Summarizing, biomass burning is a significant contributor to CH_3Cl over Africa, but our measurements show ample evidence of noncombustion sources explaining the observed high CH_3Cl mixing ratios over southern Africa. Satellite measurements also showed that seasonal variations of CH_3Cl and CO in the UT over southern and central Africa are noticeably different [*Santee et al*., 2013], being consistent with the contributions of noncombustion sources discussed above.

According to the data classification based on the back trajectory analyses and CH_3Cl to CO correlations, air samples plausibly influenced by biomass burning were identified to examine $\Delta CH_3Cl/\Delta CO$ ratios for African biomass burning (closed squares in Figures 4h–4n). Here the air samples dominantly contributed by noncombustion, and fossil fuel-related sources were excluded (open squares). Emission ratios estimated as slopes of such sub–data sets for biomass burning ranged from 0.49 to 0.82 ppt ppb^{-1}. These values fall within a range of previous measurements for biomass burning in Africa (0.50–0.95 ppt ppb^{-1}) (Table 1 and reference therein).

4.4. Variations Over South Asia

From April to December 2008, we conducted flights to Chennai (MAA; 12.99°N, 80.18°E), India, and were able to observe temporal variations of various trace gases, including CH_3Cl and CO, between Germany and India, represented in 5° latitude bins in Figure 5. The CO variation along the flight tracks has been discussed in previous papers [*Schuck et al*., 2010; *Baker et al*., 2012] and is shown here for comparison. As found over Europe and the Atlantic, but here even more clearly, the UT CH_3Cl level is higher as a whole compared to those at MHD and MLO (gray lines in Figure 5) at any observation latitudes. The other distinct feature is that elevated mixing ratios are observable between 20°–40°N during summer in association with the Asian summer monsoon. Concerning the CO mixing ratio, previous observations have shown that, reflecting the geographical distribution of CO sources, the CO mixing ratio generally increases toward the NH high latitudes [*Novelli et al*., 1998] and decreases with altitude over NH midlatitudes [*Yashiro*, 2007]. In line with this, the CO level at MHD is higher than that at MLO over the course of the year (Figure 5). The CARIBIC data show that, except for the monsoon season, the CO mixing ratios in the UT are comparable to those at MLO at lower latitudes and are intermediate between MLO and MHD at midlatitudes.

The CH_3Cl and CO mixing ratios along the South Asian flights are subsequently shown as a function of latitude in Figures 6a and 6b. The CH_3Cl mixing ratio along the flight track increases southward except in the summer monsoon season (June–September) when elevated values appear at 20°–40°N. With respect to the CO mixing ratio, high values centered at 20°–40°N also appear in the summer monsoon period, while, in the other seasons, CO decreases southward from Europe (40°–50°N) to around 30°N and then increases southward at latitudes south of 30°N (over India). At the northernmost latitudes (over eastern Europe), the relatively high CO values are presumably due to mixture of the UT air with CO-rich air masses in the LT at midlatitudes. At the southernmost latitudes, back trajectory analyses indicate that, in all observation months, the sampled air masses originated in the lower level atmosphere over southerly areas in Southeast/East Asia or partly in East Africa [*van Velthoven*, 2014]. Springtime biomass burning in Southeast Asia or urban emissions in Southeast/East Asia might contribute to the observed high CO mixing ratios.

5. Discussion

5.1. Vertical and Latitudinal Gradient of the Atmospheric CH_3Cl

The most distinct feature over Europe (Figure 1) is that CH_3Cl in the UT is significantly higher than at MHD. The annual averages of the CARIBIC (MPIC) and MHD data give a difference of 64 ± 8 ppt for the period 2008–2011. This suggests a persistent positive vertical gradient of CH_3Cl throughout the year. Similarly, ground-based

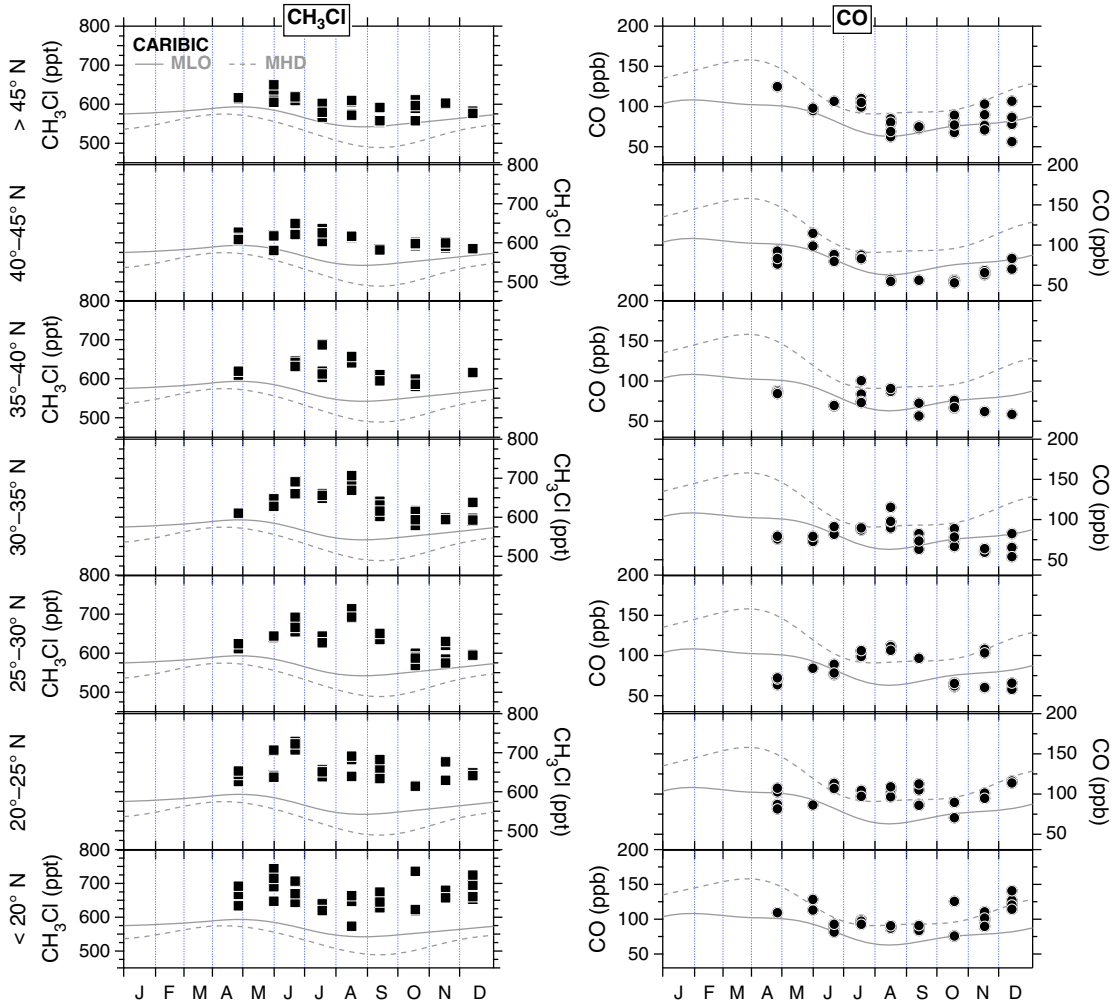

Figure 5. Time series of (left) CH_3Cl and (right) CO in the UT at 5° latitude bins obtained from the South Asian flight series between Germany and Chennai (MAA), India, in 2008. Also shown are best fit curves for NOAA flask data at MHD (dashed lines) and MLO (solid lines) for comparison. The NOAA flask CO data are from *Novelli and Masarie* [2013].

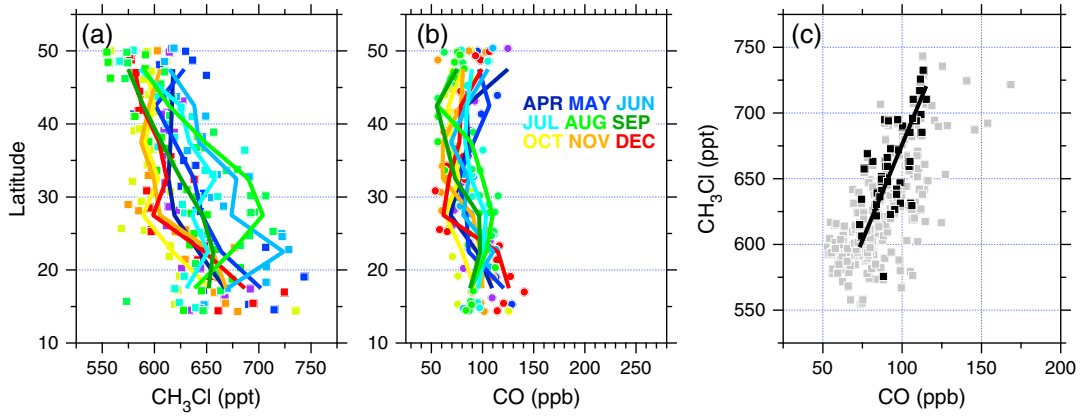

Figure 6. Latitudinal distributions of (a) CH_3Cl and (b) CO mixing ratios in the UT along the MAA flights in different months. Colors of symbols represent the observation months. (c) Scatterplots of CH_3Cl versus CO. Subset of data from air samples collected in the monsoon anticyclone is shown in black. Also shown is a geometric mean regression line for the monsoon samples.

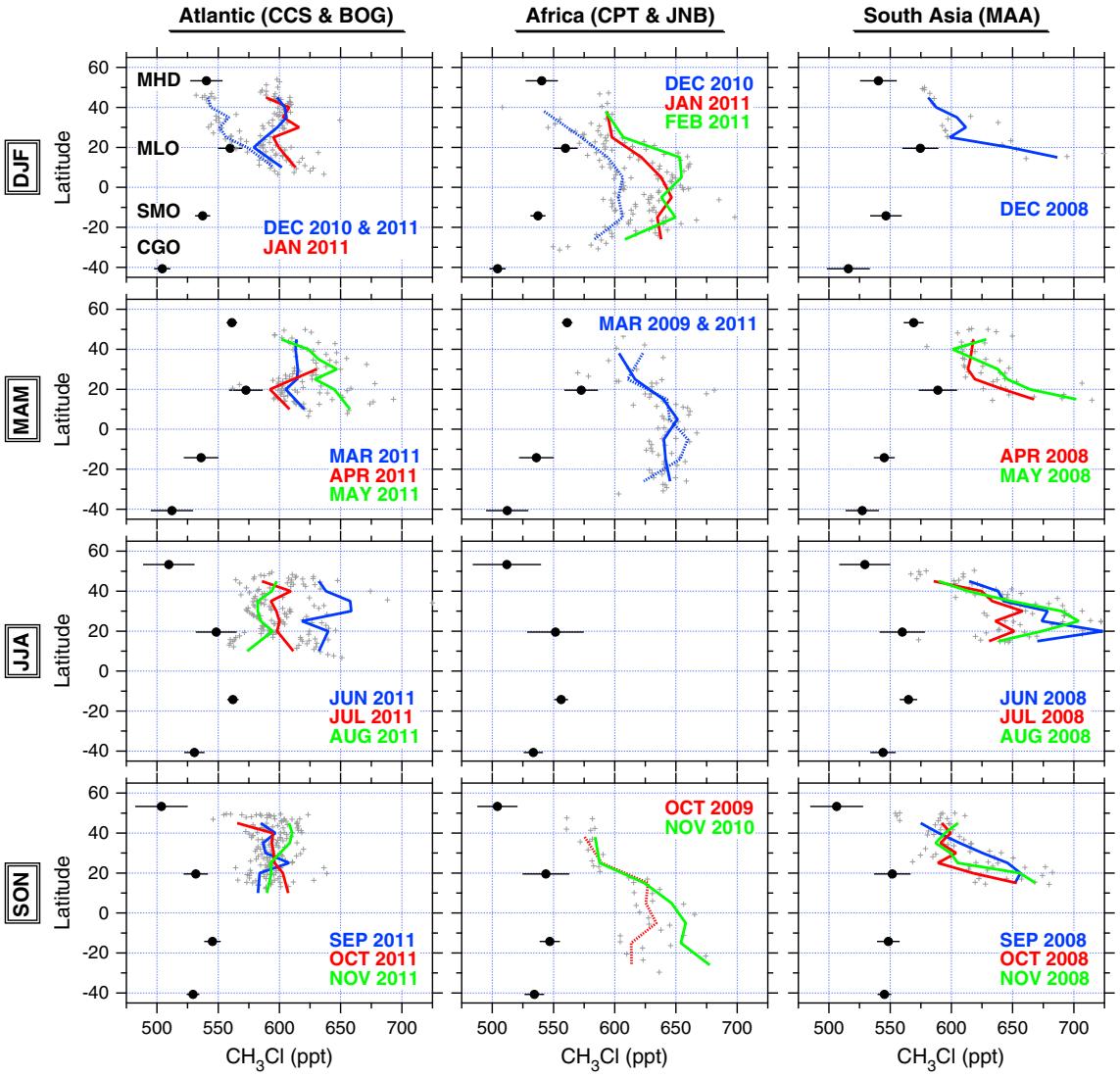

Figure 7. Latitudinal distributions of the CH_3Cl mixing ratio over the (left) Atlantic, (middle) Africa, and (right) South Asia in different seasons (DJF = December, January, February; MAM = March, April, May; JJA = June, July, August; and SON = September, October, November). The profile for the preceding year is shown by a dotted line when those in different years are plotted in one panel. The CARIBIC raw data are shown by gray crosses. The CARIBIC data were collected most frequently at altitudes of 9–12 km, and the stratosphere-influenced samples are excluded. Also shown for comparison are values derived from flasks collected at the NOAA surface measurement sites (MHD, MLO, SMO, and CGO) averaged for the CARIBIC observation period. Note that the MLO observatory is located at relatively high altitude (3433 m asl).

NOAA/ESRL-HATS flask measurements show that the annual mean CH_3Cl mixing ratio at high-altitude site Summit, Greenland (72.60°N, 38.42°W, 3220 m asl), is 16 ± 1 and 17 ± 1 ppt higher than those at other high-latitude but low-altitude sites at Alert, Canada (82.45°N, 62.51°W, 210 m asl), and Barrow, Alaska (71.32°N, 156.61°W, 27 m asl), respectively. In addition, the CH_3Cl mixing ratio observed at the high mountain site Jungfraujoch (46.55°N, 7.99°E, 3580 m asl), Switzerland, is also ~20 ppt higher than that at MHD (http://agage.eas.gatech.edu/data.htm). These station measurements are consistent with a persistent positive vertical gradient in CH_3Cl at NH midlatitudes.

The CARIBIC data suggest positive vertical gradients over wide geographical regions in both hemispheres. In Figure 7, latitudinal distributions of the CH_3Cl over the Atlantic (flights from/to CCS and BOG), Africa (from/to CPT and JNB), and South Asia (from/to MAA) in different seasons are presented in comparison with NOAA/ESRL-HATS measurements at remote surface sites. For comparison, the NOAA data were averaged for the periods corresponding to the CARIBIC flights shown in the respective panels. This figure shows that the

UT CH_3Cl level found by CARIBIC is persistently higher than those at the remote surface sites at any observation latitude over the all observation regions, with exceptions of a few flight series (for instance December 2010 over the Atlantic and Africa). It is noted that only measurements at remote surface sites (MHD, MLO, SMO, and CGO) longitudinally distant from the CARIBIC observation locations are available for comparison, and the flask samples from these sites are not directly influenced by local CH_3Cl sources throughout the year [*Yoshida et al*., 2004]. In contrast, over regions with strong CH_3Cl sources including Africa and South Asia [e.g., *Yoshida et al*., 2004], the vertical gradient might be different, and thus, one should keep in mind that Figure 7 does not represent the vertical gradient for each region.

Recently, observations by the HIPPO project [*Wofsy et al*., 2012] provided extensive CH_3Cl data sets mainly over the Pacific from five flight missions during 2009–2011 that covered all four seasons. Those measurements, conducted from flasks analyzed at NOAA and University of Miami and from an in situ instrument, also show a general positive vertical gradient at NH midlatitudes (not shown here, but data sets are available through their website http://hippo.ucar.edu). NOAA/ESRL-HATS's regular aircraft measurement programs [*Montzka et al*., 2007] have also indicated a positive vertical gradient over North America (S. Montzka, unpublished data, 2013).

However, the positive vertical gradient of the CH_3Cl mixing ratio discussed here has not been documented so far since the aforementioned systematic data sets have become available only recently. Most previous aircraft observations took place sporadically and focused on capturing pollution outflow of biomass/biofuel burning and/or industry emissions, where the persistent positive vertical gradient at midlatitudes might have been masked by such disturbances. Among previous aircraft missions, the Tropospheric Ozone Production about the Spring Equinox experiment, which was conducted at middle- to high-latitudes over North America during February–May 2000, showed slightly increasing profiles of CH_3Cl with altitude; the CH_3Cl values at ~8 km were higher by up to ~50 ppt (monthly mean values) than those near the surface [*Yoshida et al*., 2004, and references therein]. The Mediterranean Intensive Oxidant Study campaign conducted over the Mediterranean in August 2001 also reported elevated CH_3Cl values in the UT, which were attributed to transport of air polluted by biomass/biofuel burning from South Asia [*Lelieveld et al*., 2002; *Scheeren et al*., 2003b]. Another example was observed at midlatitudes over the western Pacific during Pacific Exploratory Mission-West Phase A conducted in February–March 1994 [*Blake et al*., 1997]. They showed that the CH_3Cl mixing ratios observed in the UT were higher than in the LT at latitudes north of 25°N and attributed the higher CH_3Cl values in the UT to typhoon-driven fast vertical transport of the marine boundary layer air over the Pacific. Aircraft observations during the First Aerosol Characterization Experiment also showed a positive vertical gradient over NH high latitudes [*Blake et al*., 1999]. Other aircraft observations conducted from the subtropics into the SH showed almost uniform vertical profiles from the surface to the UT, while elevated CH_3Cl values were observed in the lowermost layers over regions under influence of biogenic, industrial, and biomass burning emissions [see *Yoshida et al*., 2004].

In Figure 7, the NOAA observations show that atmospheric CH_3Cl in the clean remote air in the LT at lower latitudes are higher in all seasons, as has been reported previously [*Khalil and Rasmussen*, 1999; *Yokouchi et al*., 2000]. It is also obvious that the CH_3Cl mixing ratios vary seasonally with seasonal minima in boreal (austral) late summer in the NH (SH). As discussed earlier, a clear latitudinal gradient was not always obvious over the Atlantic (see also Figure 3). This might be ascribed to the fact that most air masses sampled over the Atlantic represent baseline air without recent contact with possible source regions influencing this gradient. In contrast, UT CH_3Cl shows clear southward increases over Africa and South Asia in the NH and reaches average values of 634 ± 5 ppt at 10°N–10°S over Africa and 660 ± 6 ppt south of 20°N over South Asia. Over Africa, active biomass burning around the equator as well as emissions from noncombustion sources in the SH are inferred to be responsible for the latitudinal distributions (Figure 4). Over South Asia, the southward increase was found in all seasons except June–September when the monsoon plume superimposes on the latitudinal gradient. It is worth mentioning that the latitudinal gradient pattern of the CO mixing ratio over South Asia is totally different from that of CH_3Cl (Figure 6). This likely reflects the presence of strong noncombustion CH_3Cl sources at lower latitudes that emit little CO and, potentially, the greater loss of CO at low latitudes owing to higher OH density.

The following scenario would explain the persistent positive vertical gradient and latitudinal gradient of atmospheric CH_3Cl. (1) No strong regional/local sources of CH_3Cl exist at midlatitudes [*Lee-Taylor et al*., 2001; *Yoshida et al*., 2004; *Xiao et al*., 2010], resulting in relatively low CH_3Cl mixing ratios in the LT over the region.

(2) In the tropics where a large fraction of CH_3Cl emissions takes place (tropical vegetation and biomass burning), active convection efficiently uplifts CH_3Cl-rich surface air to the UT. (3) Subsequent meridional transport through the UT delivers the tropical CH_3Cl-rich air to the midlatitude UT, building the positive vertical gradient as well as northward negative gradient of the CH_3Cl mixing ratio. Many studies have focused on air transport mechanisms from the viewpoint of tracer distributions, and for instance, *Miyazaki et al*. [2008] examined the role of transport processes in the tropospheric distributions of CO_2. Our observation is consistent with the conceptual picture of large-scale tropospheric transport, given CH_3Cl-specific source/sink distributions; both are active in the tropics. It should be emphasized that the positive vertical and negative northward latitudinal gradient are specific to CH_3Cl.

5.2. Monsoon Plume Over South Asia

As described in the previous sections, we observed correlations between the CH_3Cl and CO mixing ratios over the Atlantic, Africa, and South Asia, indicating contributions of burning sources. Enhancement ratios calculated from the CARIBIC data are listed in Table 1. This table shows that the $\Delta CH_3Cl/\Delta CO$ ratios for biomass burning in South America and Africa (0.49–0.93 ppt ppb^{-1}) are in good agreement with previous measurements [*Rudolph et al*., 1995; *Andreae et al*., 1996; *Blake et al*., 1996; *Andreae et al*., 2001]. In contrast, the enhancement ratio determined from the Asian summer monsoon (2.9 ± 0.5 ppt ppb^{-1}) is much higher. Previously, a modeling study indicated that a lower $\Delta CH_3Cl/\Delta CO$ ratio of 0.57 ppt ppb^{-1} [*Lobert et al*., 1999] at the South Asian sources, which was identical to that applied for the other regions, underestimated observations conducted in the South Asian outflow [*Yoshida et al*., 2004].

Enhanced vertical transport of surface air during the summer monsoon increases mixing ratios of various gases in the monsoon anticyclone in the UT over South Asia [*Schuck et al*., 2010; *Baker et al*., 2011, 2012]. Figure 5 shows that the seasonal monsoon enhancements are found in both CH_3Cl and CO at 20°–40°N; they increase from April, peak in August, and decay after that. This indicates that common sources contribute to these concomitant CH_3Cl and CO increases. The probable sources in South Asia are biomass/biofuel burning such as domestic biofuel burning and agricultural waste burning [*Lelieveld et al*., 2001; *Scheeren et al*., 2002]. It is thought that a high Cl content in fuel biomass in the region causes the largest CH_3Cl emissions from biomass burning in the world [*Lobert et al*., 1999].

We observed a linear relationship between CH_3Cl and CO mixing ratios from measurements made in the monsoon anticyclone (Figure 6c). The subset of air samples collected within the anticyclone identified by means of meteorological analyses and backward trajectories [*Baker et al*., 2012] gives a slope of CH_3Cl over CO of 2.9 ± 0.5 ppt ppb^{-1} ($R^2 = 0.40$). As discussed earlier, we consider the $\Delta CH_3Cl/\Delta CO$ ratio to represent the emission ratio of the combined source in South Asia using the assumptions that air in the monsoon anticyclone represents fresh outflow from the region [*Baker et al*., 2011, 2012] and that the effect of destruction by OH during transport is minor.

A recent inventory, the Regional Emission inventory in Asia (REAS), indicates that in India CO emissions by burning fuel in the domestic sector are the largest (55%), followed by those from industry (25%) and road transport (13%) for the year 2008 [*Kurokawa et al*., 2013]. In India, biofuel use contributes most (96%) of the domestic sector emissions with coal and other fuels playing minor roles. Biofuel combustion emits significant amounts of CH_3Cl depending on the Cl content in the material burned [*Lobert et al*., 1999], while CH_3Cl emissions from fossil fuel consumption would be minor due to relatively small emission factors [*McCulloch et al*., 1999; *Keene et al*., 1999]. We therefore infer that the $\Delta CH_3Cl/\Delta CO$ ratio obtained in this study represents an emission ratio for mainly domestic biofuel combustion in South Asia. Another possible source is open biomass burning including agricultural waste burning, but its contribution is unlikely, since biomass burning in India peaks in April and in October (two major harvest seasons), and is effectively suppressed in the wet summer monsoon season when our observation took place [*Venkataraman et al*., 2006; *Giglio et al*., 2013].

Previously, the Indian Ocean Experiment aircraft campaign over the Indian Ocean captured polluted outflow from South Asia in early spring, giving a $\Delta CH_3Cl/\Delta CO$ ratio of 1.74 ± 0.21 ppt ppb^{-1} [*Scheeren et al*., 2002]. This value is significantly lower than ours. Two factors would control emissions of CH_3Cl from combustion sources: the fuel Cl content and burning phase. Concerning the former, agricultural residues and cow dung have high Cl contents [*Lobert et al*., 1999] and they occupy substantial fraction (~20%) of various household fuel burning in India (particularly in rural areas) [*Venkataraman et al*., 2010]. With respect to the

burning phase, reduced compounds including CH_3Cl and CO are emitted mainly in the smoldering phase under incomplete combustion [e.g., *Lobert et al*., 1999]. Low combustion efficiency in Indian traditional cooking stoves leads to larger amounts of reduced compounds, and they are under ongoing replacement with advanced ones [*Venkataraman et al*., 2010]. Any changes in these complex processes might have brought the difference of the $\Delta CH_3Cl/\Delta CO$ ratio between both studies. For instance, relative contributions of various burning sources might have changed over a season.

One could speculate that vegetative CH_3Cl emissions were higher in summer (our observation season) than in spring when *Scheeren et al*. [2002] conducted their observations, possibly contributing to the difference of the $\Delta CH_3Cl/\Delta CO$ ratio. To our knowledge, however, no studies have examined seasonal change of vegetative CH_3Cl emissions in South Asia (or also in the other regions), although inverse modeling studies have inferred the summertime enhancement on continental to hemispheric scales [*Yoshida et al*., 2006; *Xiao et al*., 2010]. It is also noted that rice paddies, which are one of the typical land uses in South Asia, have no clear seasonal pattern in CH_3Cl emissions [*Redeker et al*., 2000], while coastal salt marshes emit larger amounts of CH_3Cl in summer [*Rhew et al*., 2000]. At present, this potential contribution to the observed difference of the $\Delta CH_3Cl/\Delta CO$ ratio cannot be quantified.

A compilation study for emission factors of biomass burning gives $\Delta CH_3Cl/\Delta CO$ ratios of 0.28–0.50 ppt ppb^{-1} for biofuel burning and 1.45 ± 0.82 ppt ppb^{-1} for agricultural waste burning [*Andreae and Merlet*, 2001]. An inventory study on emissions of Cl-containing compounds employed 0.57 ppt ppb^{-1} [*Lobert et al*., 1999]. These values are considerably smaller than ours; however, we note that their estimates relied mainly on measurements in Africa and North America, where burned materials have a low Cl content, and that very limited measurements using fuel biomass burned in South Asia are available [*Lobert et al*., 1999]. Besides, laboratory experiments with various fuel types have reported wide range of $\Delta CH_3Cl/\Delta CO$ ratio (0.18–4.4 ppt ppb^{-1}) [*Lobert et al*., 1991], which covers the value obtained in this study. In addition, very high $\Delta CH_3Cl/\Delta CO$ values (4–5 ppt ppb^{-1}) have also been found in smoke samples from African savanna fires, although the limited number of samples did not allow a robust estimate [*Andreae et al*., 1996].

The REAS estimated CO emissions from the domestic sector in India to be 33.9 Tg yr^{-1} with no significant seasonality for 2008 [*Kurokawa et al*., 2013]. According to the CO-based estimate employing the $\Delta CH_3Cl/\Delta CO$ ratio [*Lobert et al*., 1999; *Scheeren et al*., 2002], we estimate the annual CH_3Cl emission from domestic biofuel combustion in India to be 125 ± 21 Gg Cl yr^{-1}. Additional CO would be emitted from open biomass burning, which releases 2.5 Tg yr^{-1} of CO mainly during the nonmonsoon period according to the Global Fire Emission Database version 3.2 [*van der Werf et al*., 2010]. This CO emission would be equivalent to 9 ± 2 Gg Cl yr^{-1} if we assume the identical emission ratio, i.e., materials being burned for open biomass burning and domestic biofuel burning are the same or at least similar. Accordingly, we estimate annual CH_3Cl emission in India to be 134 ± 23 Gg Cl yr^{-1}.

Based on the same method, *Scheeren et al*. [2002] estimated CH_3Cl emission by biofuel combustion in India and surrounding countries to be 103 Gg Cl yr^{-1}, which is smaller than our estimate. Two factors should be considered for the difference from our result. First, they employed a smaller $\Delta CH_3Cl/\Delta CO$ ratio as discussed earlier. Second, they employed the EDGAR database (version 2.0) [*Olivier et al*., 1996] for CO data in 1990 that gave biofuel CO emissions of 47.2 Tg yr^{-1}. This is higher than the value we used for India but comparable if we also take into account values for the other countries in South Asia. Therefore, the different emission estimates between both studies are dominantly ascribed to the difference in the measured $\Delta CH_3Cl/\Delta CO$ ratio. Emissions of CH_3Cl from South Asia might have been underestimated, but further studies focusing on $\Delta CH_3Cl/\Delta CO$ emission ratios for various fuel types in South Asia are needed for better quantifying the CH_3Cl emissions in the region.

We also note that the REAS inventory estimates secular increase of biofuel burning in South Asia [*Ohara et al*., 2007; *Kurokawa et al*., 2013]. Although the CH_3Cl emission in India estimated in the present study comprises only less than 5% of the globally total CH_3Cl sources [e.g., *Xiao et al*., 2010] and no sustained increase of the atmospheric CH_3Cl has been observed at any monitoring stations in the remote atmosphere [*Montzka et al*., 2011b], continuing increase of biofuel burning in South Asia may cause an efficient supply of more Cl into the stratosphere through the Asian summer monsoon as an important pathway to the stratosphere [*Randel et al*., 2010].

6. Conclusion

We analyzed CH_3Cl variations observed in the UT by the CARIBIC observatory. Our measurements and comparisons with surface site data indicate that the CH_3Cl mixing ratio increases with altitude at midlatitudes and that it increases toward lower latitudes in both UT and LT of both hemispheres. These features in spatial variations are specific to CH_3Cl and likely explained by strong CH_3Cl sources in the tropics as well as global-scale transport in the troposphere. In other words, strong sources in the tropics and outflow of the tropical air to the extratropics plausibly control the global-scale distribution of CH_3Cl, implying that CH_3Cl could be a helpful tracer to identify outflow of tropical air masses. Concurrently measured CO data also suggest that the large-scale CH_3Cl distribution is maintained by emissions from noncombustion sources in the tropics, while biomass burning also plays a significant role over Africa. In the summertime monsoon plume encountered along the flights to South Asia, we observed a significant CH_3Cl to CO relationship with a slope of 2.9 ± 0.5 ppt ppb^{-1}, indicative of contribution of burning sources. Domestic biofuel burning in South Asia is inferred to play a dominant role in CH_3Cl emissions, and we estimated the emission in India to be 134 ± 23 Gg Cl yr^{-1}. This estimate is higher than a previous one due to the higher emission ratio observed in this study. South Asia may become a significant future Cl supplier to the stratosphere if the secular increase of biofuel burning continues. Since a large portion of CH_3Cl sources distributed in the tropics are not well sensed by existing surface measurement networks, the CARIBIC data in the UT will be useful to better constrain the global CH_3Cl budget by being incorporated in atmospheric chemistry transport models.

Acknowledgments

We are grateful to Lufthansa Airlines and Fraport for their support of the CARIBIC project, and we thank the CARIBIC team members. CARIBIC is part of IAGOS, and we acknowledge funding from the German Ministry of Education and Research (BMBF). The CARIBIC data are available to other parties. We acknowledge J. Elkins and B. Hall for NOAA N_2O data, P. Novelli for CO data at the NOAA surface stations, C. Siso for assistance in analyzing NOAA flasks for CH_3Cl, and B. Hall for calibration. We also thank additional members of the HIPPO team (particularly E. Atlas, F. Moore, B. Miller, and S. Wofsy) for providing their data.

References

Andreae, M. O., and P. Merlet (2001), Emission of trace gases and aerosols from biomass burning, *Global Biogeochem. Cycles*, *15*(4), 955–966, doi:10.1029/2000GB001382.

Andreae, M. O., et al. (1996), Methyl halide emissions from savanna fires in southern Africa, *J. Geophys. Res.*, *101*(D19), 23,603–23,613, doi:10.1029/95JD01733.

Andreae, M. O., et al. (2001), Transport of biomass burning smoke to the upper troposphere by deep convection in the equatorial region, *Geophys. Res. Lett.*, *28*(6), 951–954, doi:10.1029/2000GL012391.

Assonov, S. S., C. A. M. Brenninkmeijer, T. Schuck, and T. Umezawa (2013), N_2O as a tracer of mixing stratospheric and tropospheric air based on CARIBIC data with applications for CO_2, *Atmos. Environ.*, doi:10.1016/j.atmosenv.2013.07.035.

Baker, A. K., F. Slemr, and C. A. M. Brenninkmeijer (2010), Analysis of non-methane hydrocarbons in air samples collected aboard the CARIBIC passenger aircraft, *Atmos. Meas. Tech.*, *3*, 311–321, doi:10.5194/amt-3-311-2010.

Baker, A. K., T. J. Schuck, F. Slemr, P. van Velthoven, A. Zahn, and C. A. M. Brenninkmeijer (2011), Characterization of non-methane hydrocarbons in Asian summer monsoon outflow observed by the CARIBIC aircraft, *Atmos. Chem. Phys.*, *10*, 11,503–11,518, doi:10.5194/acp-11-503-2011.

Baker, A. K., T. J. Schuck, C. A. M. Brenninkmeijer, A. Rauthe-Schöch, F. Slemr, P. F. J. van Velthoven, and J. Lelieveld (2012), Estimating the contribution of monsoon-related biogenic production to methane emissions from South Asia using CARIBIC observations, *Geophys. Res. Lett.*, *39*, L10813, doi:10.1029/2012GL051756.

Blake, N. J., D. R. Blake, B. C. Sive, T.-Y. Chen, and F. S. Rowland (1996), Biomass burning emissions and vertical distribution of atmospheric methyl halides and other reduced carbon gases in the South Atlantic region, *J. Geophys. Res.*, *101*(D19), 24,151–24,164, doi:10.1029/96JD00561.

Blake, N. J., D. R. Blake, T.-Y. Chen, J. E. Collins Jr., G. W. Sachse, B. E. Anderson, and F. S. Rowland (1997), Distribution and seasonality of selected hydrocarbons and halocarbons over the western Pacific basin during PEM-West A and PEM-West B, *J. Geophys. Res.*, *102*(D23), 28,315–28,331, doi:10.1029/97JD02538.

Blake, N. J., et al. (1999), Aircraft measurements of the latitudinal, vertical, and seasonal variations of NMHCs, methyl nitrate, methyl halides, and DMS during the First Aerosol Characterization Experiment (ACE 1), *J. Geophys. Res.*, *104*(D17), 21,803–21,817, doi:10.1029/1999JD900238.

Blei, E., C. J. Hardacre, G. P. Mills, K. V. Heal, and M. R. Heal (2010), Identification and quantification of methyl halide sources in a lowland tropical rainforest, *Atmos. Environ.*, *44*, 1005–1010, doi:10.1016/j.atmosenv.2009.12.023.

Bousquet, P., et al. (2011), Source attribution of the changes in atmospheric methane for 2006–2008, *Atmos. Chem. Phys.*, *11*, 3689–3700, doi:10.5194/acp-11-3689-2011.

Brenninkmeijer, C. A. M., et al. (2007), Civil aircraft for the regular investigation of the atmosphere based on an instrumented container: The new CARIBIC system, *Atmos. Chem. Phys.*, *7*, 4953–4976, doi:10.5194/acp-7-4953-2007.

Gebhardt, S., A. Colomb, R. Hofmann, J. Williams, and J. Lelieveld (2008), Halogenated organic species over the tropical South American rainforest, *Atmos. Chem. Phys.*, *8*, 3185–3197, doi:10.5194/acp-8-3185-2008.

Giglio, L., J. T. Randerson, and G. R. van der Werf (2013), Analysis of daily, monthly, and annual burned area using the fourth-generation global fire emissions database (GFED4), *J. Geophys. Res. Biogeosci.*, *118*, 317–328, doi:10.1002/jgrg.20042.

Guenther, A., T. Karl, P. Harley, C. Wiedinmyer, P. I. Palmer, and C. Geron (2006), Estimates of global terrestrial isoprene emissions using MEGAN (Model of Emissions of Gases and Aerosols from Nature), *Atmos. Chem. Phys.*, *6*, 3181–3210, doi:10.5194/acp-6-3181-2006.

Hall, B. D., G. S. Dutton, and J. W. Elkins (2007), The NOAA nitrous oxide standard scale for atmospheric observations, *J. Geophys. Res.*, *112*, D09305, doi:10.1029/2006JD007954.

Holloway, T., H. Levy II, and P. Kasibhatla (2000), Global distribution of carbon monoxide, *J. Geophys. Res.*, *105*(D10), 12,123–12,147, doi:10.1029/1999JD901173.

Hoor, P., H. Fischer, L. Lange, J. Lelieveld, and D. Brunner (2002), Seasonal variations of a mixing layer in the lowermost stratosphere as identified by the CO-O_3 correlation from in situ measurements, *J. Geophys. Res.*, *107*(D5), 4044, doi:10.1029/2000JD000289.

Hu, L., S. A. Yvon-Lewis, J. H. Butler, J. M. Lobert, and D. B. King (2013), An improved oceanic budget for methyl chloride, *J. Geophys. Res. Oceans*, *118*, 715–725, doi:10.1029/2012JC008196.

Ishijima, K., et al. (2010), Stratospheric influence on the seasonal cycle of nitrous oxide in the troposphere as deduced from aircraft observations and model simulations, *J. Geophys. Res.*, *115*, D20308, doi:10.1029/2009JD013322.

Keene, W. C., et al. (1999), Composite global emissions of reactive chlorine from anthropogenic and natural sources: Reactive Chlorine Emissions Inventory, *J. Geophys. Res.*, *104*(D7), 8429–8440, doi:10.1029/1998JD100084.

Keppler, F., D. B. Harper, T. Röckmann, R. M. Moore, and J. T. G. Hamilton (2005), New insight into the atmospheric chloromethane budget gained using stable carbon isotope ratios, *Atmos. Chem. Phys.*, *5*, 2403–2411, doi:10.5194/acp-5-2403-2005.

Khalil, M. A. K., and R. A. Rasmussen (1999), Atmospheric methyl chloride, *Atmos. Environ.*, *33*, 1305–1321, doi:10.1016/S1352-2310(98)00234-9.

Khalil, M. A. K., and R. A. Rasmussen (2000), Soil-atmosphere exchange of radiatively and chemically active gases, *Environ. Sci. Pollut. Res.*, *7*(2), 79–82, doi:10.1065/espr2000.04.021.

Krol, M. C., J. Lelieveld, D. E. Oram, G. A. Sturrock, S. A. Penkett, C. A. M. Brenninkmeijer, V. Gros, J. Williams, and H. A. Scheeren (2003), Continuing emissions of methyl chloroform from Europe, *Nature*, *421*, 131–135, doi:10.1038/nature01311.

Kurokawa, J., T. Ohara, T. Morikawa, S. Hanayama, G. Janssens-Maenhout, T. Fukui, K. Kawashima, and H. Akimoto (2013), Emissions of air pollutants and greenhouse gases over Asian regions during 2000–2008: Regional Emission inventory in ASia (REAS) version 2, *Atmos. Chem. Phys.*, *13*, 11,019–11,058, doi:10.5194/acp-13-11019-2013.

Lai, S. C., et al. (2010), Pollution events observed during CARIBIC flights in the upper troposphere between South China and the Philippines, *Atmos. Chem. Phys.*, *10*, 1649–1660, doi:10.5194/acp-10-1649-2010.

Lai, S. C., A. K. Baker, T. J. Schuck, F. Slemr, C. A. M. Brenninkmeijer, P. van Velthoven, D. E. Oram, A. Zahn, and H. Ziereis (2011), Characterization and source regions of 51 high-CO events observed during Civil Aircraft for the Regular Investigation of the Atmosphere Based on an Instrument Container (CARIBIC) flights between south China and the Philippines, 2005–2008, *J. Geophys. Res.*, *116*, D20308, doi:10.1029/2011JD016375.

Lee-Taylor, J. M., G. P. Brasseur, and Y. Yokouchi (2001), A preliminary three-dimensional global model study of atmospheric methyl chloride distributions, *J. Geophys. Res.*, *106*(D24), 34,221–34,233, doi:10.1029/2001JD900209.

Lelieveld, J., et al. (2001), The Indian Ocean experiment: Widespread air pollution from South and Southeast Asia, *Science*, *291*, 1031–1036, doi:10.1126/science.1057103.

Lelieveld, J., et al. (2002), Global air pollution crossroads over the Mediterranean, *Science*, *298*, 794–799, doi:10.1126/science.1075457.

Lobert, J. M., D. H. Scharffe, W.-M. Hao, T. A. Kuhlbusch, R. Seuwen, P. Warneck, and P. J. Crutzen (1991), Experimental evaluation of biomass burning emissions: Nitrogen and carbon containing compounds, in *Global Biomass Burning: Atmospheric, Climatic and Biospheric Implications*, edited by J. S. Levine, pp. 289–304, The MIT Press, Cambridge, Mass.

Lobert, J. M., W. C. Keene, J. A. Logan, and R. Yevich (1999), Global chlorine emissions from biomass burning: Reactive Chlorine Emissions Inventory, *J. Geophys. Res.*, *104*(D7), 8373–8389, doi:10.1029/1998JD100077.

Mayaux, P., E. Bartholome, S. Fritz, and A. Belward (2004), A new land-cover map of Africa for the year 2000, *J. Biogeogr.*, *31*, 861–877, doi:10.1111/j.1365-2699.2004.01073.x.

McCulloch, A., M. L. Aucott, C. M. Benkovitz, T. E. Graedel, G. Kleiman, P. M. Midgley, and Y.-F. Li (1999), Global emissions of hydrogen chloride and chloromethane from coal combustion, incineration and industrial activities: Reactive Chlorine Emissions Inventory, *J. Geophys. Res.*, *104*(D7), 8391–8404, doi:10.1029/1999JD900025.

Miyazaki, K., P. K. Patra, M. Takigawa, T. Iwasaki, and T. Nakazawa (2008), Global-scale transport of carbon dioxide in the troposphere, *J. Geophys. Res.*, *113*, D15301, doi:10.1029/2007JD009557.

Montzka, S. A., P. Calvert, B. D. Hall, J. W. Elkins, T. J. Conway, P. P. Tans, and C. Sweeney (2007), On the global distribution, seasonality, and budget of atmospheric carbonyl sulfide (COS) and some similarities to CO_2, *J. Geophys. Res.*, *112*, D09302, doi:10.1029/2006JD007665.

Montzka, S. A., et al. (2011a), Ozone-Depleting Substances (ODSs) and related chemicals, in *Scientific Assessment of Ozone Depletion: 2010*, chap. 1, pp. 1.1–1.108, World Meteorological Organization, Geneva, Switz.

Montzka, S. A., M. Krol, E. Dlugokencky, B. Hall, P. Jöckel, and J. Lelieveld (2011b), Small interannual variability of global atmospheric hydroxyl, *Science*, *331*, 67–69, doi:10.1126/science.1197640.

Moore, R. M., W. Groszko, and S. J. Niven (1996), Ocean-atmosphere exchange of methyl chloride: Results from NW Atlantic and Pacific Ocean studies, *J. Geophys. Res.*, *101*(C12), 28,529–28,538, doi:10.1029/96JC02915.

Nakazawa, T., M. Ishizawa, K. Higuchi, and N. B. A. Trivett (1997), Two curve fitting methods applied to CO_2 flask data, *Environmetrics*, *8*, 197–218, doi:10.1002/(SICI)1099-095X(199705)8:3<197::AID-ENV248>3.0.CO;2-C.

Nedelec, P., V. Thouret, J. Brioude, B. Sauvage, J.-P. Cammas, and A. Stohl (2005), Extreme CO concentrations in the upper troposphere over northeast Asia in June 2003 from the in situ MOZAIC aircraft data, *Geophys. Res. Lett.*, *32*, L14807, doi:10.1029/2005GL023141.

Novelli, P. C., and K. A. Masarie (2013), Atmospheric carbon monoxide dry air mole fractions from the NOAA ESRL carbon cycle cooperative global air sampling network, 1988-2012, Version: 2013-06-18, Path: ftp://aftp.cmdl.noaa.gov/data/trace_gases/co/flask/surface/.

Novelli, P. C., K. A. Masarie, and P. M. Lang (1998), Distributions and recent changes of carbon monoxide in the lower troposphere, *J. Geophys. Res.*, *103*(D15), 19,015–19,033, doi:10.1029/98JD01366.

Ohara, T., H. Akimoto, J. Kurokawa, N. Horii, K. Yamaji, X. Yan, and T. Hayasaka (2007), An Asian emission inventory of anthropogenic emission sources for the period 1980–2020, *Atmos. Chem. Phys.*, *7*, 4419–4444, doi:10.5194/acp-7-4419-2007.

Olivier, J. G. J., A. F. Bouwman, C. W. M. van der Maas, J. J. M. Berdowski, C. Veldt, J. P. J. Bloos, A. J. H. Visschedijk, P. Y. J. Zandveld, and J. L. Haverlag (1996), Description of EDGAR Version 2.0: A set of global emission inventories of greenhouse gases and ozone-depleting substances for all anthropogenic and most natural sources on a per country basis and on 1°×1° grid, National Institute of Public Health and the Environment, Report 771060 002.

Prinn, R., D. Cunnold, R. Rasmussen, P. Simmonds, F. Alyea, A. Crawford, P. Fraser, and R. Rosen (1990), Atmospheric emissions and trends o nitrous oxide deduce from 10 years of ALE-GAGE data, *J. Geophys. Res.*, *95*(D11), 18,369–18,385, doi:10.1029/JD095iD11p18369.

Prinn, R. G., et al. (2000), A history of chemically and radiatively important gases in air deduced from ALE/GAGE/AGAGE, *J. Geophys. Res.*, *105*(D14), 17,751–17,792, doi:10.1029/2000JD900141.

Randel, W. J., M. Park, L. Emmons, D. Kinnison, P. Bernath, K. A. Walker, C. Boone, and H. Pumphrey (2010), Asian monsoon transport of pollution to the stratosphere, *Science*, *328*, 611–613, doi:10.1126/science.1182274.

Redeker, K. R., N.-Y. Wang, J. C. Low, A. McMillan, S. C. Tyler, and R. J. Cicerone (2000), Emissions of methyl halides and methane from rice paddies, *Science*, *290*, 966–969, doi:10.1126/science.290.5493.966.

Rhew, R. C., B. R. Miller, and R. F. Weiss (2000), Natural methyl bromide and methyl chloride emissions from coastal salt marshes, *Nature*, *403*, 292–295, doi:10.1038/35002043.

Rudolph, J., A. Khedim, R. Koppmann, and B. Bonsang (1995), Field study of the emissions of methyl chloride and other halocarbons from biomass burning in Western Africa, *J. Atmos. Chem.*, *22*, 67–80, doi:10.1007/BF00708182.

Saito, T., and Y. Yokouchi (2008), Stable carbon isotope ratio of methyl chloride emitted from glasshouse-grown tropical plants and its implication for the global methyl chloride budget, *Geophys. Res. Lett.*, *35*, L08807, doi:10.1029/2007GL032736.

Saito, T., Y. Yokouchi, Y. Kosugi, M. Tani, E. Philip, and T. Okuda (2008), Methyl chloride and isoprene emissions from tropical rain forest in Southeast Asia, *Geophys. Res. Lett.*, *35*, L19812, doi:10.1029/2008GL035241.

Sander, S. P., et al. (2011), *Chemical Kinetics and Photochemical Data for Use in Atmospheric Studies, Evaluation No. 17*, Jet Propul. Lab., Pasadena, Calif.

Santee, M. L., N. J. Livesey, G. L. Manney, A. Lambert, and W. G. Read (2013), Methyl chloride from the Aura Microwave Limb Sounder: First global climatology and assessment of variability in the upper troposphere and stratosphere, *J. Geophys. Res. Atmos.*, *118*, 1–29, doi:10.1002/2013JD020235.

Scharffe, D., F. Slemr, C. A. M. Brenninkmeijer, and A. Zahn (2012), Carbon monoxide measurements onboard the CARIBIC passenger aircraft using UV resonance fluorescence, *Atmos. Meas. Tech.*, *5*, 1753–1760, doi:10.5194/amt-5-1753-2012.

Scheeren, H. A., J. Lelieveld, J. A. de Gouw, C. van der Veen, and H. Fischer (2002), Methyl chloride and other chlorocarbons in polluted air during INDOEX, *J. Geophys. Res.*, *107*(D19), 8015, doi:10.1029/2001JD001121.

Scheeren, H. A., et al. (2003a), Reactive organic species in the northern extratropical lowermost stratosphere: Seasonal variability and implications for OH, *J. Geophys. Res.*, *108*(D24), 4805, doi:10.1029/2003JD003650.

Scheeren, H. A., et al. (2003b), The impact of monsoon outflow from India and Southeast Asia in the upper troposphere over the eastern Mediterranean, *Atmos. Chem. Phys.*, *3*, 1589–1608, doi:10.5194/acp-3-1589-2003.

Schmidt, U., D. Knapska, and S. A. Penkett (1985), A study of the vertical distribution of methyl chloride (CH_3Cl) in the midlatitude stratosphere, *J. Atmos. Chem.*, *3*, 363–376, doi:10.1007/BF00122524.

Schuck, T. J., C. A. M. Brenninkmeijer, F. Slemr, I. Xueref-Remy, and A. Zahn (2009), Greenhouse gas analysis of air samples collected onboard the CARIBIC passenger aircraft, *Atmos. Meas. Tech.*, *2*, 449–464, doi:10.5194/amt-2-449-2009.

Schuck, T. J., C. A. M. Brenninkmeijer, A. K. Baker, F. Slemr, P. F. J. van Velthoven, and A. Zahn (2010), Greenhouse gas relationships in the Indian summer monsoon plume measured by the CARIBIC passenger aircraft, *Atmos. Chem. Phys.*, *10*, 3965–3984, doi:10.5194/acp-10-3965-2010.

Schuck, T. J., K. Ishijima, P. K. Patra, A. K. Baker, T. Machida, H. Matsueda, Y. Sawa, T. Umezawa, C. A. M. Brenninkmeijer, and J. Lelieveld (2012), Distribution of methane in the tropical upper troposphere measured by CARIBIC and CONTRAIL aircraft, *J. Geophys. Res.*, *117*, D19304, doi:10.1029/2012JD018199.

Simmonds, P. G., et al. (2004), AGAGE observations of methyl bromide and methyl chloride at Mace Head, Ireland, and Cape Grim, Tasmania, 1998–2001, *J. Atmos. Chem.*, *47*, 243–269, doi:10.1023/B:JOCH.0000021136.52340.9c.

Spivakovsky, C. M., et al. (2000), Three-dimensional climatological distribution of tropospheric OH: Update and evaluation, *J. Geophys. Res.*, *105*(D7), 8931–8980, doi:10.1029/1999JD901006.

Thouret, V., J.-P. Cammas, B. Sauvage, G. Athier, R. Zbinden, P. Nédélec, P. Simon, and F. Karcher (2006), Tropopause referenced ozone climatology and inter-annual variability (1994–2003) from the MOZAIC programme, *Atmos. Chem. Phys.*, *6*, 1033–1051, doi:10.5194/acp-6-1033-2006.

van der Werf, G. R., J. T. Randerson, L. Giglio, G. J. Collatz, M. Mu, P. S. Kasibhatla, D. C. Morton, R. S. DeFries, Y. Jin, and T. T. van Leeuwen (2010), Global fire emissions and the contribution of deforestation, savanna, forest, agricultural, and peat fires (1997–2009), *Atmos. Chem. Phys.*, *10*, 11,707–11,735, doi:10.5194/acp-10-11707-2010.

van Velthoven, P. F. J. (2014), Meteorological analysis of CARIBIC by KNMI. [Available at http://www.knmi.nl/samenw/campaign_support/CARIBIC/.]

Venkataraman, C., G. Habib, D. Kadamba, M. Shrivastava, J.-F. Leon, B. Crouzille, O. Boucher, and D. G. Streets (2006), Emissions from open biomass burning in India: Integrating the inventory approach with high-resolution Moderate Resolution Imaging Spectroradiometer (MODIS) active-fire and land cover data, *Global Biogeochem. Cycles*, *20*, GB2013, doi:10.1029/2005GB002547.

Venkataraman, C., A. D. Sagar, G. Habib, N. Lam, and K. R. Smith (2010), The Indian National Initiative for Advanced Biomass Cookstoves: The benefits of clean combustion, *Energy Sustain. Dev.*, *14*, 63–72, doi:10.1016/j.esd.2010.04.005.

Wofsy, S. C., et al. (2012), HIPPO combined discrete flask and GC sample GHG, halo-, hydrocarbon data (R_20121129), Carbon Dioxide Inf. Anal. Cent., Oak Ridge Natl. Lab., Oak Ridge, Tenn., doi:10.3334/CDIAC/hippo_012, (Release 20121129).

Xiao, X., et al. (2010), Optimal estimation of the surface fluxes of methyl chloride using a 3-D global chemical transport model, *Atmos. Chem. Phys.*, *10*, 5515–5533, doi:10.5194/acp-10-5515-2010.

Xiong, X., C. D. Barnet, Q. Zhuang, T. Machida, C. Sweeney, and P. K. Patra (2010), Mid-upper tropospheric methane in the high Northern Hemisphere: Spaceborne observations by AIRS, aircraft measurements, and model simulations, *J. Geophys. Res.*, *115*, D19309, doi:10.1029/2009JD013796.

Yashiro, H. (2007), A study of temporal and spatial variations of tropospheric carbon monoxide, PhD thesis, Graduate School of Science, Tohoku University, Sendai, Japan.

Yokouchi, Y., Y. Noijiri, L. A. Barrie, D. Toom-Sauntry, T. Machida, Y. Inuzuka, H. Akimoto, H.-J. Li, Y. Fujinuma, and S. Aoki (2000), A strong source of methyl chloride to the atmosphere from tropical coastal land, *Nature*, *403*(295–298), 2000, doi:10.1038/35002049.

Yokouchi, Y., M. Ikeda, Y. Inuzuka, and T. Yukawa (2002), Strong emission of methyl chloride from tropical plants, *Nature*, *416*, 163–165, doi:10.1038/416163a.

Yokouchi, Y., T. Saito, C. Ishigaki, and M. Aramoto (2007), Identification of methyl chloride-emitting plants and atmospheric measurements on a subtropical island, *Chemosphere*, *69*, 549–553, doi:10.1016/j.chemosphere.2007.03.028.

Yoshida, Y., Y. Wang, T. Zeng, and R. Yantosca (2004), A three-dimensional global model study of atmospheric methyl chloride budget and distributions, *J. Geophys. Res.*, *109*, D24309, doi:10.1029/2004JD004951.

Yoshida, Y., Y. Wang, C. Shim, D. Cunnold, D. R. Blake, and G. S. Dutton (2006), Inverse modeling of the global methyl chloride sources, *J. Geophys. Res.*, *111*, D16307, doi:10.1029/2005JD006696.

Zahn, A., and C. A. M. Brenninkmeijer (2003), New directions: A chemical tropopause defined, *Atmos. Environ.*, *37*, 439–440, doi:10.1016/S1352-2310(02)00901-9.

Zahn, A., J. Weppner, H. Widmann, K. Schlote-Holubek, B. Burger, T. Kühner, and H. Franke (2012), A fast and precise chemiluminescence ozone detector for eddy flux and airborne application, *Atmos. Meas. Tech.*, *5*, 363–375, doi:10.5194/amt-5-363-2012.